Active Sensing for Target Tracking: A Bayesian Optimisation Approach

Xingchi Liu[1,2], Lyudmila Mihaylova[1]

[1]Department of Automatic Control and Systems Engineering, University of Sheffield, Sheffield, UK
[2]Scientific Computing Department, Rutherford Appleton Laboratory, Science and Technology Facilities Council, UK
Email: xingchi.liu@stfc.ac.uk, l.s.mihaylova@sheffield.ac.uk

Abstract—Active sensing plays an essential role in searching and tracking a target without initial target state information. This paper studies the active sensing approach for sensor management problems using multiple unmanned aerial vehicles based on the received signal strength measurements of the target. A Bayesian optimisation-based approach is proposed which adopts the Gaussian process method to model the received signal strength in an area over time and then the expected improvement acquisition function is leveraged to decide where to take new measurements considering the uncertainty of the Gaussian process. A unique contribution of this paper consists of the designed spatial-temporal composite kernel function that accounts for the time-varying nature of the signal strength. Numerical results obtained from different measurement noise levels and varying initial Bayesian optimisation settings demonstrate that the proposed approach can efficiently schedule multiple unmanned aerial vehicles to locate the target within a minimum number of initial data. Particularly, it achieves at most 57% lower tracking error and 46% lower lost-track probability as compared to the benchmark approach.

Index Terms—Bayesian optimisation, target tracking, sensor management, Gaussian process, unmanned aerial vehicles, active sensing

I. INTRODUCTION

Target tracking is a fundamental task for various applications including sea surveillance, autonomous vehicles, and traffic monitoring. Both model-based and data-driven approaches have been proposed to solve related problems such as data association, sensor management, and group/extended tracking. Nevertheless, many of these works rely on informative prior beliefs of the target location, which may not be available, for instance, the target could be lost track or perform tracking in an active sensing [1], [2] scenario.

The main challenge of the above problem is how to efficiently locate the target for tracking. Track-before-detect is a well-known technology that can help to extract point measurements of the target from a large number of sensor measurements. It can improve track accuracy and allow the tracker to follow targets with a low signal-to-noise ratio [3], [4]. However, this type of technology normally requires high computational and memory costs to deal with large volumes of data. In addition, it is a model-based approach and needs the target state-space model to perform the target state estimation.

There are previous works using Bayesian optimisation (BO) to solve the searching and localisation problems. As a machine learning-based optimisation method, BO builds a surrogate model for the objective function with prediction uncertainty quantification using Gaussian process (GP) regression and iteratively locates the global optimum based on an acquisition function (AF) defined on the surrogate. BO has been applied to various searching and localisation problems, including locating WiFi devices [5], environmental monitoring [6], and contaminant source identification [7]. In [5], GP was used to model the received signal strength (RSS) of a smartphone in a certain area as a map. Applying BO, the position of the highest RSS was located within just a few minutes using an unmanned aerial vehicle (UAV). In [6], a BO approach is applied to generate the actions of a moving robot to measure the ozone concentration to substitute a large number of sensor nodes for monitoring. In [7], BO solved the problem of searching for the contaminant source, by modelling the concentration of the contaminant in a certain area using GP. However, most existing works focused on searching for static targets, which means they modelled the observations from stationary functions using GP without considering the dynamics of the functions.

BO can also be used to solve dynamic and non-stationary optimisation problems. In [8], a warping function was introduced to convert a stationary kernel into a non-stationary one. Then the data will follow a stationary process in the transferred space. There was also work [9] studying to partition the data space into sub-spaces and modelled each region as a separate stationary process. Furthermore, [10] proposed a combination of local and global GPs to account for the non-stationary process and solve the non-stationary optimisation problems. Although these works have been demonstrated to succeed in various applications, they did not explicitly consider the time dependencies of the observations. In [11], a spatial-temporal kernel was designed to model the function over time, thereby solving the dynamic optimisation problem with BO.

A. Main Contributions

This paper proposes a BO-guided active sensing approach to manage sensors to search and track a moving target. Different from our previous work [12] where we track in a distributed way, this work focuses on tracking in an active manner without prior position information. The proposed approach is based on RSS measurements which is a popular type of data for tracking [13]. In particular, GP has been applied to learn the RSS map

of the target in an area of interest area [5], [14], [15]. The main contribution consists of the developed spatial-temporal composite kernel functions to account for the time-varying and non-stationary nature of the RSS map. Moreover, it can schedule multiple UAVs to accelerate the searching process and maintain robustness in high-noise scenarios. The proposed approach can also be applied to determine sensor activation over time in sensor management problems [16], to save power and reduce received clutter measurements.

Particularly, the algorithms proposed in this paper differs from our previous work [17] in several aspects: 1) the previous work focused on efficient GP factorisation approaches for BO, while in this work, we propose a composite kernel design to represent the target dynamics. This kernel function characterises the local stationarity of the time-varying RSS map in a more accurate manner. 2) a thorough validation of the proposed approaches is performed over a range of case studies with varying numbers of sensors and different levels of sensor measurement noise.

The rest of the paper is organised as follows. Section II introduces the problem formulations and the fundamentals of BO. Section III describes the proposed BO-guided searching and tracking approach. The simulation results are presented in Section IV, followed by the conclusions in Section V.

II. PROBLEM FORMULATION

We first model the RSS of a moving target as a black-box function of the coordinates of the measuring location and the time. Define the location of measuring the RSS in time t as $\mathbf{x}_t \in \mathcal{X} \subset \mathbb{R}^2$, where $\mathcal{X}$ is the area of interest. Denote y as the measurement, a black-box dynamic function can be written as

$$y = f(\mathbf{x}_t, t) + \epsilon, \tag{1}$$

where ϵ is the measurement noise. The noise follows a zero-mean Gaussian distribution with variance σ^2.

Given the fact that the expected value of an RSS measurement increases as the distance between the target and the receiver decreases, the location corresponding to the highest expected value of the RSS measurements is treated as the target location. Therefore, the problem of searching and tracking a target over time becomes finding the maximum of the black-box dynamic function, which is a dynamic optimisation problem [18]. This optimisation problem can be formulated as

$$(\mathcal{P}) \ \max \ f(\mathbf{x}_t, t), \tag{2}$$
$$\textbf{s.t.} \ \mathbf{x}_t \in \mathcal{X}, \ t \in \mathcal{T}, \tag{3}$$

where $\mathcal{X}$ and $\mathcal{T}$ are the spatial and temporal search spaces, respectively.

In the following sections, we leverage the GP to model this black-box function. Then, AF is used to determine where to place the UAVs to measure the signal strengths of the target in a sequential way to optimise the objective function online.

A. Gaussian Process Regression

Since the unknown function $f(\mathbf{x}_t, t)$ is a black-box function with no analytical form available, GP is used as a surrogate model of the function for the following reasons: 1) GP can quantify the uncertainty of the learned knowledge of RSS values in a principled way, which provides useful information to balance the exploration-exploitation (EE) tradeoff for solving the maximisation problem (see more details in the next section). 2) GP works well with a small volume of data and is especially useful in the early stage of the searching process where only a limited number of RSS measurements is available to build the surrogate. The GP that is placed as a prior distribution of the unknown function $f(\mathbf{x}_t, t)$ can be written as

$$f(\mathbf{x}_t, t) \sim \mathcal{GP}\left(m(\mathbf{x}_t, t), k((\mathbf{x}_t, t), (\mathbf{x}'_t, t'))\right), \tag{4}$$

where $(\mathbf{x}_t, t)$ and $(\mathbf{x}'_t, t')$ are either the training or the testing input data. $m(\mathbf{x}_t, t)$ and $k((\mathbf{x}_t, t), (\mathbf{x}'_t, t'))$ denote the mean and the covariance functions of GP, respectively.

Suppose that by the time t, n_t RSS measurements have been received with time stamps $t_1, t_2, \cdots, t_{n_t}$. Define $\mathbf{x}_{t_i}$ as the location associated with the measurement at time stamp t_i, where $t_i \leq t$. In addition, define y_{t_i} as the RSS measurement at t_i. Therefore, at any time t, we can have a set of 3-tuple that can be denoted as $\mathcal{D}_t = \{\mathbf{x}_{t_i}, t_i, y_{t_i}\}_{i=1}^{n_t}$.

Given $\mathcal{D}_t$, define $\mathbf{K}_t$ as a covariance matrix with the $(i, j)^{\text{th}}$ entry as $k((\mathbf{x}_{t_i}, t_i), (\mathbf{x}_{t_j}, t_j))$. In addition, define $\mathbf{k}_*$ as a vector with the jth entry as $k((\mathbf{x}_{t_j}, t_j), (\mathbf{x}_{t_*}, t_*))$. Denote the set of measurements received until time t by $\mathbf{y}_t = [y_{t_1}, y_{t_2}, \cdots, y_{t_{n_t}}]^{\mathsf{T}}$. The GP regression equations at a new input $(\mathbf{x}_*, t_*)$ can be written as

$$\mu_* = m(\mathbf{x}_*, t_*) + \mathbf{k}_*^{\mathsf{T}}(\mathbf{K}_t + \sigma^2\mathbf{I})^{-1}(\mathbf{y}_t - m(\mathbf{x}_*, t_*)), \tag{5}$$
$$\sigma_*^2 = k((\mathbf{x}_*, t_*), (\mathbf{x}_*, t_*)) - \mathbf{k}_*^{\mathsf{T}}(\mathbf{K}_t + \sigma^2\mathbf{I})^{-1}\mathbf{k}_*, \tag{6}$$

where μ_* and σ_*^2 denote the posterior predictive mean and variance of the unknown function at $(\mathbf{x}_*, t_*)$, respectively.

The hyperparameters of GP need to be learned from the data. As a standard GP, maximum likelihood estimation is applied to learn the hyperparameters by maximising the log marginal likelihood which can be written as

$$\log p(\mathbf{y}_t | \mathcal{D}_t, \boldsymbol{\theta}) = -1/2 \mathbf{y}_t^{\mathsf{T}}(\mathbf{K}_t + \sigma^2\mathbf{I})^{-1}\mathbf{y}_t$$
$$- 1/2 \log|\mathbf{K}_t + \sigma^2\mathbf{I}| - n_t/2 \log 2\pi, \tag{7}$$

where $\boldsymbol{\theta}$ represents the set of hyperparameters.

B. Acquisition Function

After building a surrogate model of the unknown function, the challenge is how to sequentially select measuring points to evaluate the unknown function (collect RSS measurements), thereby finding the maximum RSS value and locating the moving target efficiently (e.g. with a minimum number of measurements). There exists an EE dilemma in this decision-making process: If keeping exploring the unknown function to gain knowledge, some low RSS measurements will be collected, resulting in low searching efficiency. However, only
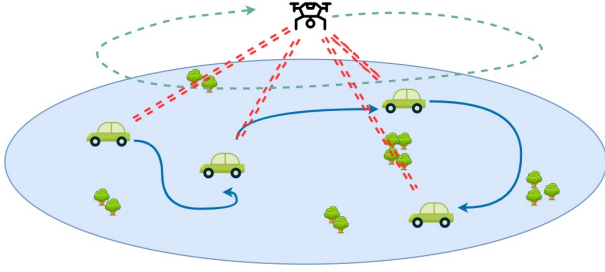
Fig. 1. UAV-assisted target searching and tracking

Fig. 2. RSS map at a certain time

exploiting the learned knowledge could miss the opportunity to receive higher RSS from under-explored areas. Therefore, in this section, we optimise an AF [19] to determine the measuring points. The AF is a function of the learned RSS map and its uncertainty from the surrogate. It provides a principled way to balance the EE and guide the optimisation process.

1) Expected improvement: The choice of AF represents different strategies for choosing the next measuring point. Here we apply the widely used expected improvement (EI) function [20]. Define an incumbent measurement $\tau_{n_t} = \max_{i \in \{1,2,\cdots,n_t\}} \mathbf{y}_{t_i}$. The aim is to find the next measuring point which gives the highest EI of RSS as compared to the incumbent measurement. The EI function can be written as

$$\alpha_{\text{EI}}(\mathbf{x}_t, t) := \mathbb{E}[[f(\mathbf{x}_t, t) - \tau_{n_t}]^+],$$
$$= \sigma(\mathbf{x}_t, t)\phi\left(\frac{\Delta(\mathbf{x}_t, t)}{\sigma(\mathbf{x}_t, t)}\right) + \Delta(\mathbf{x}_t, t)\Phi\left(\frac{\Delta(\mathbf{x}_t, t)}{\sigma(\mathbf{x}_t, t)}\right), \quad (8)$$

where $\Delta(\mathbf{x}_t, t) = \mu(\mathbf{x}_t, t) - \tau_{n_t}$, is the expected difference between the predictive RSS at a point and the incumbent target. Here $\phi(\cdot)$ and $\Phi(\cdot)$ denote the probability density and cumulative density functions, respectively. $\mathbb{E}(\cdot)$ represents the mathematical expectation operation. In (8), the predictive standard deviation affects the value of the first term and the predictive mean affects the second term. By maximizing the EI function, the EE tradeoff can be well-balanced.

III. BO-GUIDED TARGET TRACKING USING UAVS

To search and track a moving target as presented in Fig (1), we assume UAVs equipped with RSS sensors can fly over the region of interest and measure the RSS from the target. Since we intend to search for a moving target and only highly limited data can be collected over time, how to build the surrogate model (GP) to accurately reflect the learned knowledge of the dynamic function $f(\mathbf{x}_t, t)$ becomes a crucial challenge. In this section, the kernel design of GP is discussed.

A. Kernel Function Design

Inspired by [11], a spatial-temporal kernel function is designed to capture both the spatial the temporal correlations in the unknown time-varying function. This kernel function can be written as

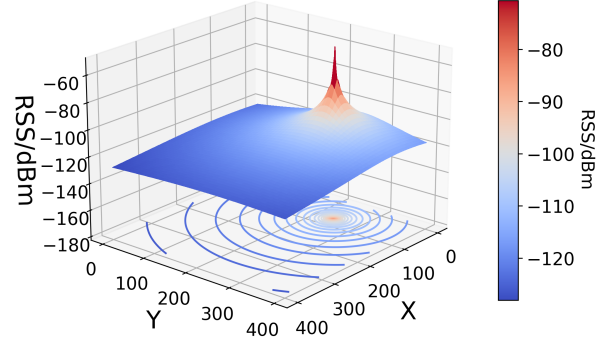$$k((\mathbf{x}_t, t), (\mathbf{x}'_t, t')) = k_{\text{S}}(\mathbf{x}_t, \mathbf{x}'_t) \cdot k_{\text{T}}(t, t'), \quad (9)$$

where $k_{\text{S}}(\cdot, \cdot)$ represents the spatial kernel, used for capturing the one-time RSS map. $k_{\text{T}}(\cdot, \cdot)$ represents the temporal kernel which reflects the correlation of the RSS maps over time.

Particularly, considering a large area of interest, at one time stamp, the RSS map of the target can be almost flat in most regions that are far from the true location of the target. Therefore, the RSS may only become high and vary a lot in a relatively small region, which is more informative in order to maximise the unknown function. In Fig 2, an RSS map of a 400 meters × 400 meters area is presented, with the highest strength located at (80,250). This map is generated using the log distance path loss model, the details of this model will be given in Section IV-A. This figure shows that based on the path loss model, the RSS in a certain area is a local stationary process [10] even without considering time correlation. Therefore, a single stationary kernel will not capture the behaviour of this process.

In this paper, we design a composite kernel as the spatial kernel to characterise the local stationarity of the RSS map. The spatial kernel is defined as a sum of a constant kernel $k_{\text{S,Con}}$, a squared exponential (SE) kernel $k_{\text{S,SE}}$, and an exponential kernel $k_{\text{S,Exp}}$. The constant kernel is added considering the fact that the RSS values in a certain area are all above a certain number. The SE kernel represents the smooth changes of RSS in most of the area (the blue area in Fig 2). To account for the rapid RSS changes around the informative area (the red area in Fig 2), we also added an exponential kernel. For the temporal kernel, we choose to use Matérn kernel $k_{\text{T,Mat}}$ since it includes a large class of kernels and is proven to be very useful for matching physical processes more realistically because of this flexibility.

The kernel function (9) can be rewritten as

$$k((\mathbf{x}_t, t), (\mathbf{x}'_t, t')) = (k_{\text{S,Con}}(\mathbf{x}_t, \mathbf{x}'_t)$$
$$+ k_{\text{S,SE}}(\mathbf{x}_t, \mathbf{x}'_t) + k_{\text{S,Exp}}(\mathbf{x}_t, \mathbf{x}'_t)) \cdot k_{\text{T,Mat}}(t, t'), \quad (10)$$
$$k_{\text{S,Con}}(\mathbf{x}_t, \mathbf{x}'_t) = \Phi, \quad (11)$$
$$k_{\text{S,SE}}(\mathbf{x}_t, \mathbf{x}'_t) = \sigma_m^2 \exp\left(-\|\mathbf{x}_t - \mathbf{x}'_t\|^2/l^2\right), \quad (12)$$
$$k_{\text{S,Exp}}(\mathbf{x}_t, \mathbf{x}'_t) = \sigma_m^2 \exp\left(-\|\mathbf{x}_t - \mathbf{x}'_t\|/l\right), \quad (13)$$

$$k_{\text{T,Mat}}(t, t') = \sigma_m^2 \frac{2^{1-v}}{\Gamma(v)} \left(\frac{\sqrt{2v}\|t - t'\|}{l}\right)^v K_v\left(\frac{\sqrt{2v}\|t - t'\|}{l}\right), \tag{14}$$

where σ_m^2 and l are the amplitude and length scale parameters, respectively. Φ represents a constant. $k_v(\cdot)$ is a modified Bessel function and $\Gamma(\cdot)$ is a Gamma function. Moreover, v is a smoothness parameter of Matérn kernel. Different functions belonging to the Matérn kernel can be built with varying v.

Algorithm 1 BO-guided active sensing

Require: Prior surrogate model $\mathcal{GP}_0$, initial data $\mathcal{D}_0$, UAV number K

1: **while** $t_i \leq T$ **do**
2:     Receive the K RSS measurements
3:     Set the time stamp $t_i = \max\{t_i^1, t_i^2, \cdots, t_i^K\}$
4:     Augment data $\mathcal{D}_i \leftarrow \mathcal{D}_{i-1} \cup \left\{\mathbf{x}_{t_i}^k, t_i^k, y_{t_i}^k\right\}_{k=1}^K$
5:     Update $\mathcal{GP}_i$ by maximising (7)
6:     Set the start time stamp $t_s \leftarrow t_i + \psi$
7:     Update search bound of time scale as $\mathbf{t} = [t_s, t_s + \gamma]$
8:     Determine $\{\mathbf{x}_{t_{i+1}}^k\}_{k=1}^K$ and $\{t_{i+1}^k\}_{k=1}^K$ by sequentially maximising AF as follows:

$$\{\mathbf{x}_{t_{i+1}}^k, t_{i+1}^k\} = \arg\max_{\mathbf{x}_t \in \mathcal{X}, t \in \mathbf{t}} \alpha^k(\mathbf{x}_t, t)$$

9:     Send the UAVs to measure the RSSs at $\{\mathbf{x}_{t_{i+1}}^k, t_{i+1}\}_{k=1}^K$
10:    $i \leftarrow i + 1$
11: **end while**

B. Multi-Agent BO

In practice, using more than one UAV to measure the signal strength can collect more data for GP update and capture the temporal correlation more efficiently. Selecting multiple measuring points belongs to the parallel BO problem [19]. One straightforward solution is to consider a multi-point EI (q-EI) scheme. Despite this, there is no closed form of the q-EI when $q > 2$, and searching for the globally optimal vector of points can be computationally intensive. Therefore, we consider an approximated q-EI that uses a sequential standard EI as a replacement [21]. This scheme chooses the measuring point sequentially following (8), assuming that the RSS value of the previous point has already been observed, which equals a constant (usually the predictive mean of the unknown dynamic function $f(\cdot)$ is used). Based on the approximated q-EI, the complexity of solving the EI function only grows linearly in terms of the number of agents (UAVs).

C. Algorithm Overview

As discussed in previous sections, BO-guided tracking employs a GP prior $\mathcal{GP}_0$ as the surrogate model of the unknown dynamic function, along with an initial set of data $\mathcal{D}_0$. The initial data can be randomly sampled from the search space representing an area of interest of the target location $\mathbf{x}$ and a period of time $\mathbf{t}$. Subsequently, the GP is used to construct the AF, guiding the searching for the target location associated with the maximum RSS over time.

Initial data	Number of UAVs	Spatial kernel	$\sigma = 1.0$ dB	$\sigma = 5.0$ dB
10	1	Con+SE	101.03(36/100)	139.57(55/100)
		Con+SE+Exp	43.28 (5/100)	86.34(22/100)
	2	Con+SE	27.67(1/100)	59.16(13/100)
		Con+SE+Exp	24.60(0/100)	37.20(5/100)
	3	Con+SE	25.67(0/100)	32.99(2/100)
		Con+SE+Exp	18.21(0/100)	24.87(1/100)
30	1	Con+SE	57.58(15/100)	130.91(59/100)
		Con+SE+Exp	32.53(1/100)	68.22(13/100)
	2	Con+SE	29.30(2/100)	41.57(4/100)
		Con+SE+Exp	25.02(2/100)	28.56(0/100)
	3	Con+SE	24.13(1/100)	32.65(3/100)
		Con+SE+Exp	17.32(0/100)	20.82(0/100)

In addition, at any time t_i, define the spatial search space as the whole area of interest and the temporal search space as $\mathbf{t} = [t_s, t_s + \gamma]$, where $t_s = t_i + \psi$. The parameters γ and ψ can be adjusted to constrain the temporal search space by controlling how far the algorithm can look forward in the time domain to decide when to take measurements. This will help to alleviate the myopic issue of the EI function.

The proposed algorithm works in an iterative process, the UAVs are scheduled to collect measurements and send the measurements to an edge node which then updates GP and determines new points for UAVs to measure. The proposed algorithm will terminate after a pre-defined time period T. The detailed process is described in Algorithm 1. We introduce a superscript $k \in 1, 2, \cdots K$ to represent different UAVs, where K is the number of UAVs.

IV. NUMERICAL RESULTS

A. Observation Model

A commonly used radio propagation model for the wireless channel is the log distance path loss model [22]. This model considers the path loss that a signal encounters inside a building or densely populated areas over a distance. In addition, it also takes attenuation caused by flat fading into account. In all simulations, the log distance path loss model is used to generate RSS measurements of the moving target. The RSS of a target received by a UAV can be written as

$$y_{t_i} = y_{0,t_i} - \eta \log_{10}(d_{t_i}) + \epsilon, \tag{15}$$

where d_{t_i} represents the distance between the target and the UAV at t_i. y_{0,t_i} is a constant characterising the transmission power of the UAV at t_i with the unit of dBm; η is a slope index; ϵ is the logarithm of the shadowing component, which is assumed to be a zero mean Gaussian noise. The proposed algorithm is validated by setting the standard deviation of the Gaussian noise as 1 and 5 dB in the RSS measurements.

B. Simulation Settings

The performance of the proposed approach is tested in a 400 meters $\times$ 400 meters area. The target trajectory is generated based on the constant velocity model with the initial target

(a) $n_t = 0$

(b) $n_t = 30$
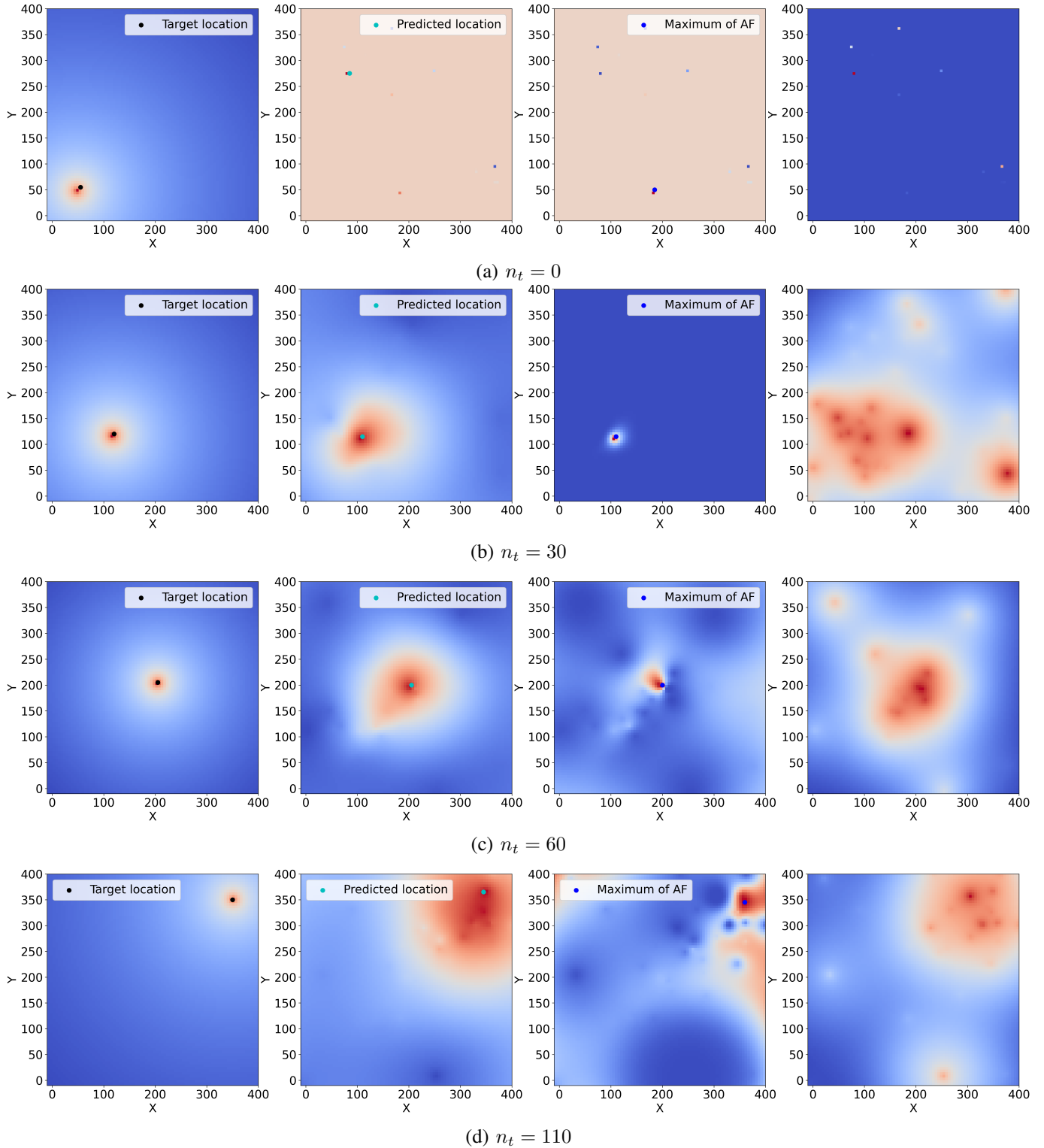
(c) $n_t = 60$

(d) $n_t = 110$

Fig. 3. Ground truth RSS map, learned RSS surrogate, value of AF, and uncertainty estimation of surrogate based on increasing number of collected RSS measurements. Each row represents a different number of received RSS measurements n_t in the process. The red region represents higher RSS values in the first and second figure of each subfigure. The red region also represent the high AF values and high predictive confidence in the third and fourth subfigures, respectively.
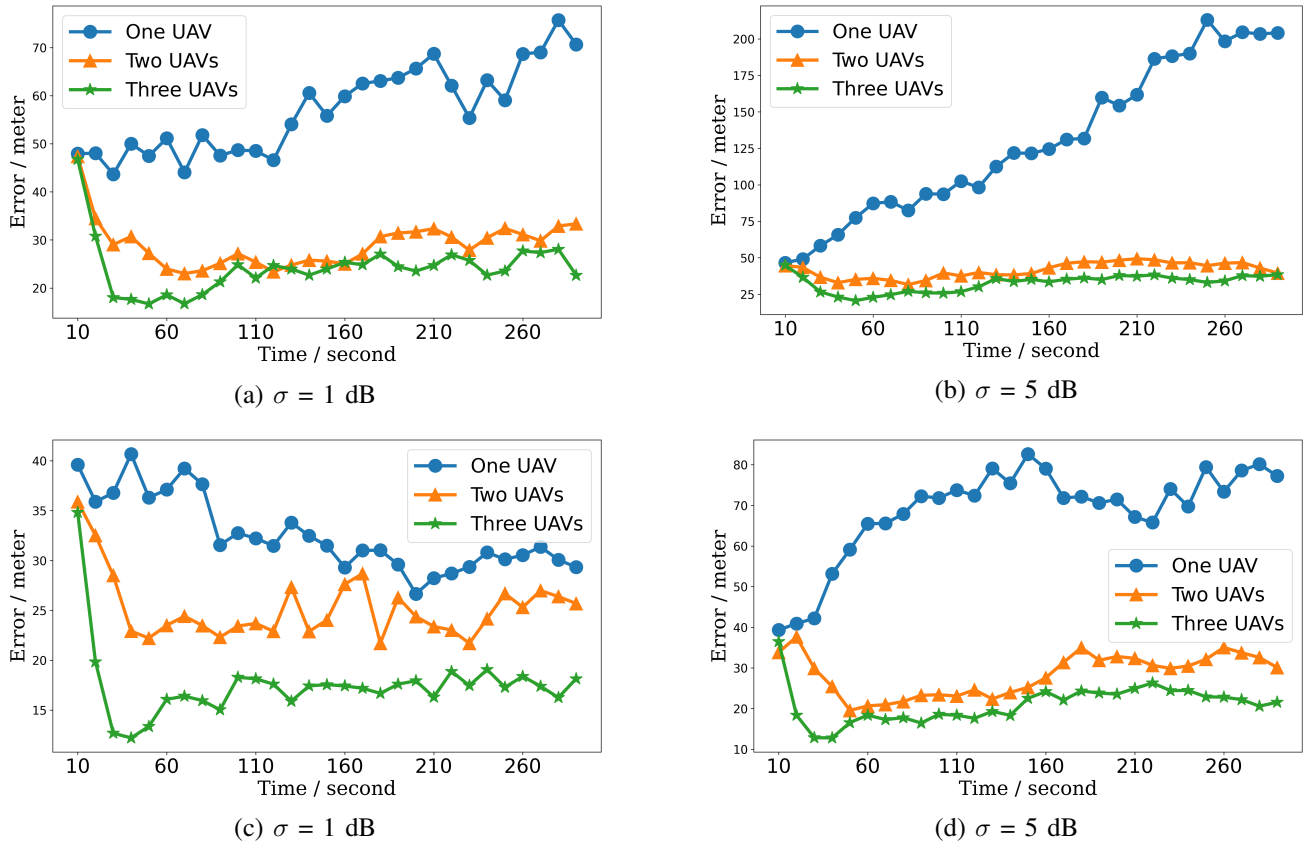
Fig. 4. Target location prediction error versus time, $|\mathcal{D}_0| = 30$. The performance of the benchmark scheme is presented in (a) and (b) using spatial kernel $k_S = k_{S,\text{Con}} + k_{S,\text{SE}}$. The performance of the proposed algorithm is presented in (c) and (d) using the designed kernel function in (10)

state vector $[50m, 1m/s, 50m, 1m/s]$. The proposed algorithm is compared with a benchmark algorithm presented in [11], which uses BO to solve dynamic optimisation problems. We set $\psi = 1, \gamma = 2$ to construct the temporal search space.

C. Tracking Process Visualisation

The searching and tracking process of the proposed algorithm using a single UAV with 10 initial data is visualised in Fig 3. Each row of the figures, from left to right, presents the true RSS map of the experimental region, the predictive mean RSS of the posterior GP, the value of the acquisition function, and the predicted uncertainty of the GP surrogate, at different times. The point with the maximum AF value is the location to which the UAV is dispatched for measurement collection.

Fig 3 (a) presents the results at the very early stage of the searching and tracking process. The predicted target location is notably distant from the true target location due to the limited knowledge learned at this point. In the third subfigure of (a), it is evident that the UAV is scheduled to a location far from the predicted target location, indicating that our scheme is actively searching for the target to reduce the uncertainty of the surrogate model and has yet to accumulate sufficient information for accurate prediction. The low confidence can also be observed in the last figure of Fig 3 (a), displaying

a substantial predictive uncertainty across the entire region. From Fig 3 (b), as more measurements are collected for GP update, the proposed algorithm becomes increasingly accurate, and the UAV is scheduled to move around the target. This illustrates that the algorithm successfully narrows down the target location to a smaller region with higher confidence.

D. Tracking Error and Robustness

The prediction errors of the two approaches are presented in Table I with varying numbers of UAVs, initial data sizes, and measurement noise levels. The tracking error is defined as the mean Euclidean distance between the predicted target locations and the true locations. The results are further averaged over 100 Monte Carlo simulations. The empirical probability of lost track is also calculated to show how many simulations the approaches fail to track the target. We determine a case to be lost track if the tracking accuracy remains higher than a threshold when the simulation terminates. This probability can serve as a metric of robustness. The table reveals that the proposed approach can work on a very limited size of initial data and efficiently utilize multiple UAVs for searching and tracking. With more UAVs implemented, both the tracking error and the empirical probability of lost track can be reduced.

E. Impact of Kernel Function Design

Table I also describes the impact of having different types of spatial kernels in the proposed and benchmark approaches. Overall, the proposed approach using the designed spatial kernel outperforms the benchmark with lower error, higher reliability and efficient resource allocation. In particular, when only one UAV is used, having an extra exponential kernel function achieves at most 57% lower tracking error and improves with 31% the tracking robustness in the low-noise case, as compared to the benchmark. In the high-noise case, it helps to achieve at most 48% lower tracking error and improves with 46% the tracking robustness. The results demonstrate that the designed composite kernel can better account for the local stationarity of the RSS map. Fig 4 presents the averaged prediction errors with varying numbers of UAVs over time. The designed spatial kernel with three components performs better in all the cases. As compared to the benchmark, the proposed approach with the designed spatial kernel (10) achieves noteworthy error reduction when having measurements from two and three UAVs.

V. Conclusion

This paper proposes a novel active sensing approach to manage several UAVs to search and track a moving target using RSS measurements. To model the dynamic nature of the latent process of the RSS generation over time, a spatial-temporal composite kernel is designed to build a GP surrogate model for the process. The effectiveness of the proposed approach is evaluated based on varying measurement levels and initial settings. The proposed approach with a combination of kernels - constant, exponential, and SE kernels can help BO to efficiently locate the target. Particularly, it achieves at most 57% and 48% lower tracking error than approaches with other kernels in low and high-noise cases, respectively. Future research could be carried out to extend BO for multi-target searching and tracking problems.

Acknowledgement

References

[1] L. Varotto, A. Cenedese, and A. Cavallaro, "Active sensing for search and tracking: A review," *arXiv preprint arXiv:2112.02381*, 2021.

[2] C. Kreucher, K. Kastella, and A. O. Hero III, "Sensor management using an active sensing approach," *Signal Processing*, vol. 85, no. 3, pp. 607–624, 2005.

[3] S. J. Davey, M. G. Rutten, and B. Cheung, "A comparison of detection performance for several track-before-detect algorithms," *EURASIP J. Adv. Signal Process*, vol. 2008, no. 1, pp. 1–10, 2007.

[4] Y. Boers, H. Driessen, J. Torstensson, M. Trieb, R. Karlsson, and F. Gustafsson, "Track-before-detect algorithm for tracking extended targets," *IEE Proceedings-Radar, Sonar and Navigation*, vol. 153, no. 4, pp. 345–351, 2006.

[5] M. Carpin, S. Rosati, M. E. Khan, and B. Rimoldi, "UAVs using Bayesian optimization to locate WiFi devices," *arXiv:1510.03592*, 2015.

[6] R. Marchant and F. Ramos, "Bayesian optimisation for intelligent environmental monitoring," in *Proceedings of the IEEE/RSJ International conf. on Intelligent Robots and Systems*. IEEE, 2012, pp. 2242–2249.

[7] G. Pirot, T. Krityakierne, D. Ginsbourger, and P. Renard, "Contaminant source localization via Bayesian global optimization," *Hydrology and Earth System Sciences*, vol. 23, no. 1, pp. 351–369, 2019.

[8] J. Snoek, K. Swersky, R. Zemel, and R. Adams, "Input warping for Bayesian optimization of non-stationary functions," in *Proceedings of the 31st International Conference on Machine Learning*, 2014.

[9] R. B. Gramacy, H. K. H. Lee, and W. G. Macready, "Parameter space exploration with Gaussian process trees," in *Proceedings of the Twenty-First International Conference on Machine Learning*, 2004.

[10] R. Martinez-Cantin, "Bayesian optimization with adaptive kernels for robot control," in *Proceeding of the IEEE International Conference on Robotics and Automation*, 2017, pp. 3350–3356.

[11] F. M. Nyikosa, M. A. Osborne, and S. J. Roberts, "Bayesian optimization for dynamic problems," *arXiv preprint arXiv:1803.03432*, 2018.

[12] X. Liu, L. Mihaylova, J. George, and T. Pham, "Gaussian process upper confidence bounds in distributed point target tracking over wireless sensor networks," *IEEE Journal of Selected Topics in Signal Processing*, vol. 17, no. 1, pp. 295–310, 2023.

[13] O. Kaltiokallio, R. Hostettler, and N. Patwari, "A novel Bayesian filter for RSS-based device-free localization and tracking," *IEEE Transactions on Mobile Computing*, vol. 20, no. 3, pp. 780–795, 2021.

[14] F. Yin and F. Gunnarsson, "Distributed recursive Gaussian processes for RSS map applied to target tracking," *IEEE Journal of Selected Topics in Signal Processing*, vol. 11, no. 3, pp. 492–503, 2017.

[15] W. Sun, M. Xue, H. Yu, H. Tang, and A. Lin, "Augmentation of fingerprints for indoor WiFi localization based on Gaussian process regression," *IEEE Transactions on Vehicular Technology*, vol. 67, no. 11, pp. 10 896–10 905, 2018.

[16] A. O. Hero and D. Cochran, "Sensor management: Past, present, and future," *IEEE Sensors Journal*, vol. 11, no. 12, pp. 3064–3075, 2011.

[17] X. Liu, C. Lyu, S. A. Soleymani, W. Wang, and L. Mihaylova, "Joint sensor scheduling and target tracking with efficient bayesian optimisation," in *Proceedings of the Sensor Signal Processing for Defence Conference (SSPD)*, 2023, pp. 1–5.

[18] C. Cruz, J. R. González, and D. A. Pelta, "Optimization in dynamic environments: a survey on problems, methods and measures," *Soft Computing*, vol. 15, no. 7, pp. 1427–1448, 2011.

[19] P. I. Frazier, "A tutorial on Bayesian optimization," *arXiv preprint arXiv:1807.02811*, 2018.

[20] J. Mockus, V. Tiesis, and A. Zilinskas, "The application of Bayesian methods for seeking the extremum," *Towards global optimization*, vol. 2, pp. 117–129, 1978.

[21] D. Ginsbourger, R. Le Riche, and L. Carraro, "Kriging is well-suited to parallelize optimization," in *Computational Intelligence in Expensive Optimization Problems*, 2010, vol. 2, ch. 6, pp. 131–162.

[22] L. Mihaylova, D. Angelova, S. Honary, D. R. Bull, C. N. Canagarajah, and B. Ristic, "Mobility tracking in cellular networks using particle filtering," *IEEE Transactions on Wireless Communications*, vol. 6, no. 10, pp. 3589–3599, 2007.